N74 30931

ASM/NASA/GWU SYMPOSIUM ON

WELDING, BONDING AND FASTENING

Williamsburg, Virginia

May 30 - June 1, 1972

HIGH POWER LASER WELDING

Conrad M. Banas
Senior Research Engineer
United Aircraft Research Laboratories
East Hartford, Connecticut 06108

ABSTRACT

A review of recent developments in high-power, carbon-dixoide laser welding is presented. Deep-penetration welding in stainless steel to 0.5-in. thick, high-speed welding in thin gage rimmed steel and gas-shielded welding in Ti-6Al-4V alloy are described.

The effects of laser power, power density, focusing optics, gas-shielding techniques, material properties and weld speed on weld quality and penetration are discussed. It is shown that laser welding performance in thin materials is comparable to that of electron beams. It is further shown that high quality welds, as evidenced by NDT, mechanical and metal-lographic tests, can be achieved. The potential of the laser for industrial welding applications is indicated.

201<

INTRODUCTION

From its initial development, the laser has been hailed as a pontentially useful welding tool for a variety of applications. Until recently, however, laser welding has been restricted to relatively thin materials and low speeds by the limited power available on a continuous basis. With the development of multikilowatt, continuously-operating, CO_2 laser systems (Refs. 1-3 and Fig. 1), this limitation has been obviated and the scope of technically-feasible laser welding applications has been correspondingly broadened.

The laser's capability for generating a power density greater than 10^6 watt/in.^{2} is a primary factor in establishing its potential for welding. A power density of this magnitude can only be duplicated with electron-beam welding equipment and provides the laser with the ability to produce deep-penetration welds. As may be noted from Fig. 2, which was obtained with electron-beam equipment, a deep-penetration threshold exists at a power density of the order of 10^6 watt-in.^{2}. At low power densities, characteristic of typical gas and arc-welding equipment, a shallow, roughly-hemispherical weld zone is formed. At somewhat higher power densities, characteristic of modern plasma-arc welding equipment, a wine-glass-shaped weld zone is generated. At still higher power densities, deep penetration is achieved. By way of illustration it is noted that a power density of 10^6 watt/in.^{2} is equivalent to that provided by a thermal source at 23,000^{o}R.

The deep-penetration capability of electron beams extends only a short distance out of vacuum. By contrast, CO_2 laser beams can be transmitted for appreciable distances through the atmosphere without serious attenuation or optical degradation. In addition, laser beams may be readily directed and shaped with front-surface mirrors and they do not generate x-rays on interaction with a metallic workpiece. For these reasons the laser appears potentially more versatile for many production welding applications.

Several disadvantages of the laser relative to the electron beam may also be noted. The focused beam spot diameter is limited by diffraction to a size that is directly proportional to the radiation wavelength, λ, and the focal length of the optics and is inversely proportional to the effective aperture or beam diameter (Fig. 3). The ratio of focal length to aperture diameter is referred to as the f/number. Since the equivalent wavelength of a high-voltage electron beam is much shorter than the 10.6 micron wavelength of CO_2 laser radiation, a higher f/number, and a correspondingly longer depth of field, may be utilized to provide a given power density. As a result, surface positioning is less critical than with laser beams and penetration into thick workpieces is facilitated.

Other factors which detract from the potential of lasers for welding are that room temperature metal surface reflectivity for CO_2 laser radiation is quite high and that focused laser radiation can result in generation of a beam-absorbing plasma in the vicinity of a workpiece. Plasma formation stems from gas breakdown induced by the electric field due to the focused electromagnetic radiation (laser beam). In dry air the breakdown threshold for CO_2 laser radiation is of the order of 10^9 watt/in.^{2}. Evolution of particles and metal vapor from the workpiece during the welding process, however, can reduce this threshold to a level of the order of 10^6 watt/in.^{2} (Fig. 4). If adequate provision is not taken to eliminate breakdown, beam absorption occurs in the generated plasma and inefficient welding performance is obtained. Since breakdown parameters depend on gas type, shield gas composition for laser welding must be selected on the basis of gas-breakdown characteristics as well as on weld zone metallurgical requirements.

Investigation of the effects of the above noted factors on laser welding performance has constituted a portion of the laser materials processing program at the United Aircraft Research Laboratories. This paper has been prepared to present a review of some of the more recent developments in high-power laser welding and to provide an insight into possible near-term industrial welding applications.

EXPERIMENTAL APPARATUS AND PROCEDURE

The laser welding tests described herein were conducted with a convectively-cooled, multikilowatt, continuous, CO_2 laser. This unit, shown in Fig. 1, operates as an amplifier for a low power input beam from a stable laser oscillator. In this manner high optical output power is achieved in the fundamental (TEM_{00}) mode of laser oscillation; this facilitates focusing and thereby enhances metal working capability. The laser amplifier consists of twelve separate discharge tubes connected electrically in parallel and optically in series. High specific power per unit volume is achieved by the expedient of rapid flow of the gases through the tubes such that convective cooling of the discharge medium is achieved. The gases from the discharge tubes pass through a heat exchanger in which the waste energy from the electric discharge is removed, through a circulating pump, through a second heat exchanger which removes the heat of compression and then back through the laser channel. Recirculation of the gases permits reduction in pumping power requirements and operating cost. It is, however, necessary to continuously remove and replenish a small fraction of the circulating gas to maintain a constant composition. This requirement stems from the fact that CO_2 dissociation and formation of oxides of nitrogen are induced by the high-voltage electric discharge.

A plane mirror mounted on a solenoid-actuated slide was used to deflect the high-power beam from the amplifier into a calorimeter which served to monitor power as well as to provide an energy sink for the beam between weld passes. As shown in Fig. 5, the beam was directed toward, and focused upon, the workpiece by an 18-degree-off-axis parabolic mirror. The workpiece was placed on a variable speed table which could be moved under the focused beam at speeds ranging from 5 to 500 ipm. A modified, gas-tungsten-arc welding fixture was used to provide a protective atmosphere for reactive materials; the trailer shield of this fixture was oriented such that the laser beam passed through the opening provided for the tungsten electrode.

During a welding test, the deflecting mirror was withdrawn and the workpiece was translated beneath the focused beam at a controlled speed. Most tests were conducted with the beam focused at the workpiece surface. Inert gas shielding was provided for reactive metals; for other materials a low-velocity crossflow of inert gas was used to prevent plasma formation. Workpiece travel (and hence weld length) was limited by the fixturing to approximately 6 inches. Since laser output can readily be held constant at the multikilowatt level for hours at a time, this limitation should not be construed as a limitation of laser welding capability.

DISCUSSION OF EXPERIMENTAL WELDING RESULTS

The high power laser equipment described in the foregoing section was utilized for investigations of welding in a number of materials. The first welds were effected in 300 series stainless steel with results represented by the butt weld cross section shown in Fig. 6. The 1/4-in., deep-penetration weld shown exhibits a depth-to-width ratio of about 7:1 and was formed in atmosphere at a speed of 50 ipm and a laser power of 3.5 kW. The edges of the butt weld configuration were machined to provide close fit up so that filler material was not required. Radiographic inspection of selected stainless steel welds has shown that sound, nonporous welds can be formed. Further, tensile tests have shown that welds exhibiting a strength equivalent to that of the parent material can be generated.

A parametric representation of laser welding performance in stainless steel is shown in Fig. 7. It may be seen from Fig. 7 that penetration increases essentially in proportion to the laser power level. Also to be noted is that the maximum penetration achieved was 0.5 in. at a laser power level of 5.5 kW and a welding speed of 10 ipm. Attempts to increase penetration by decrease in welding speed resulted in collapse of the deep-penetration mode and a decrease in penetration. Figure 7 further illustrates that the depth of penetration decreases slowly with increase in welding speed. Increasing the welding speed, however, does significantly decrease the width of the weld zone such that thermal energy input and distortion are minimized. The reduction in weld zone cross section with increase in welding speed is treated in more detail in the subsequent discussion of titanium alloy welding results.

Parametric curves similar to those for stainless steel have also been generated for low-carbon, rimmed steel and are presented in Fig. 8. Once again it is noted that the depth of penetration for laser welding decreases slowly with increase in welding speed and that penetration is approximately proportional to the laser power level. The absolute level of penetration obtained is somewhat less than that for stainless steel; this may be due to the higher thermal diffusivity of rimmed steel. Of particular note is that welding speeds greater than 200 ipm were achieved in 0.1-in. thick material at power levels of the order of 4 kW. High quality welds, which exhibited a tensile strength higher than that of the parent material, were obtained provided that the mating surfaces were appropriately treated with a deoxidant. Inert gas shielding also led to a significant improvement in rimmed steel weld quality. As may be seen in Fig. 9, gas shielding completely eliminated blowhole generation in rimmed steel without use of a deoxidant at the weld zone.

Helium shielding was also utilized on the top and bottom surfaces of the Ti-6Al-4V penetrations shown in Fig. 10. The material was machined prior to test to remove surface scale, then cleaned in an acid solution, subsequently rinsed with alcohol and dried with Freon-12. Material of 0.2 in. thickness was used and a copper chill bar was positioned approximately 0.02 in. beneath the lower weld surface. It is noted from Fig. 10 that a thin, high depth-to-width ratio melt zone is formed at high welding speeds. As welding speed is decreased, conduction into the surrounding material leads to a broader melted zone and to a characteristic hourglass shape. With further decrease in welding speed the fused zone becomes still broader and nearly uniform in width throughout the entire penetration. At very low welding speeds the deep-penetration mode collapses and an extremely shallow fused zone is obtained. The faster heating and cooling rates encountered at high welding speed also tend to reduce grain growth in the weld zone as may be seen in the magnified cross sections shown in Fig. 11.

The dependence of Ti-6Al-4V penetration on welding speed and laser power is shown in Figs. 12 and 13. It is noted that the general characteristics of the relationship in Fig. 12 are similar to those for stainless and rimmed steels shown previously in Figs. 7 and 8. The somewhat lower rate of decrease in penetration with speed may be caused by the lower thermal diffusivity of titanium alloy which facilitates the generation and maintenance of a stable deep-penetration welding mode.

Initial radiographic inspection of laser welds in Ti-6Al-4V alloy has shown evidence of pinhole porosity of the type encountered in electron beam welding. Such porosity may be due to the intermittent collapse of the deep-penetration cavity and underscores the requirement for precise definition and control of welding parameters in high-beam-power-density welding of titanium alloys. Post-weld heat treating, improved gas shielding and limited fatigue endurance tests are planned for future studies.

In order to place the above described laser welding performance in proper perspective, it is useful to compare the results with electron beam data. A convenient vehicle for this comparison is the nondimensional representation formulated in Ref. 4 and utilized in Fig. 14. The nondimensional parameter on the ordinate contains the depth of penetration, b, the laser power level, P, the thermal conductivity of the material, K, and a characteristic melting temperature, T_M, which includes the heat of fusion divided by the specific heat. The parameter on the abscissa contains the thermal diffusivity of the material, α, the welding speed, V, and the incident spot size of the focused beam, d. With other parameters held constant, this representation can be considered as a curve of depth of penetration as a function of welding speed. Thus the characteristic should be, and is, similar to that for the parametric data presented for stainless steel, rimmed steel and titanium alloy in Figs. 7, 8 and 12.

Laser welding performance in aluminum, titanium, stainless steel and rimmed steel obtained to date is seen to be comparable to that for electron beams. In view of the relatively high initial surface reflectivity of metallic surfaces at 10.6 microns, it must be concluded that this reflectivity decreases essentially to zero during the deep-penetration process. It is postulated that the deep-penetration cavity serves as a black body radiation trap for the laser radiation and thus facilitates efficient laser welding. A corollary to the above conclusion relative to high welding efficiency is that plasma generation was effectively prevented in the tests reported. It should be emphasized, however, that performance comparable to electron beams may not necessarily pertain in thicker materials for which higher power levels (with attendant increased probability of breakdown) and higher f/numbers (to promote penetration) will be required.

CONCLUDING REMARKS

The welding performance which has been demonstrated, together with the unparalleled adaptability of laser welding to automation, indicates a high-potential for cost-effective, near-term industrial applications. Exploitation of this potential presently awaits the development of durable, high-power, production-oriented laser welding equipment. Recent attainment of significantly higher continuous laser power than that reported herein (Ref. 3), has substantially improved the prospects for such development.

ACKNOWLEDGEMENT

The work reported herein was performed at the United Aircraft Research Laboratories (UARL) under Corporate sponsorship. The author gratefully acknowledges the contributions of personnel of the Electric Discharge Laser Technology Section of UARL to the development of the laser used in the tests and to the performance of portions of the experimental laser welding program.

REFERENCES

1. BROWN, C. O.: High-Power, CO_2 Electric-Discharge Mixing Laser. Applied Physics Letters, Vol. 17, No. 9, November, 1970.

2. BROWN, C. O. and J. W. Davis: Electric Discharge Convection Lasers. Paper presented at the IEEE International Electron Devices Meeting, Washington, D. C., October, 1970.

3. DAVIS, J. W. and C. O. Brown: Electric-Discharge Convection Lasers: Paper 72-722, AIAA 5th Fluid and Plasma Dynamics Conference, June 26-28, 1972, Boston, Mass.

4. HABLANIAN, M. H.: A Correlation of Welding Variables, Proceedings of the 5th Symposium on Electron Beam Technology, 1963.

287<

LIST OF FIGURES

HIGH-POWER, CLOSED-CYCLE LASER TEST FACILITY

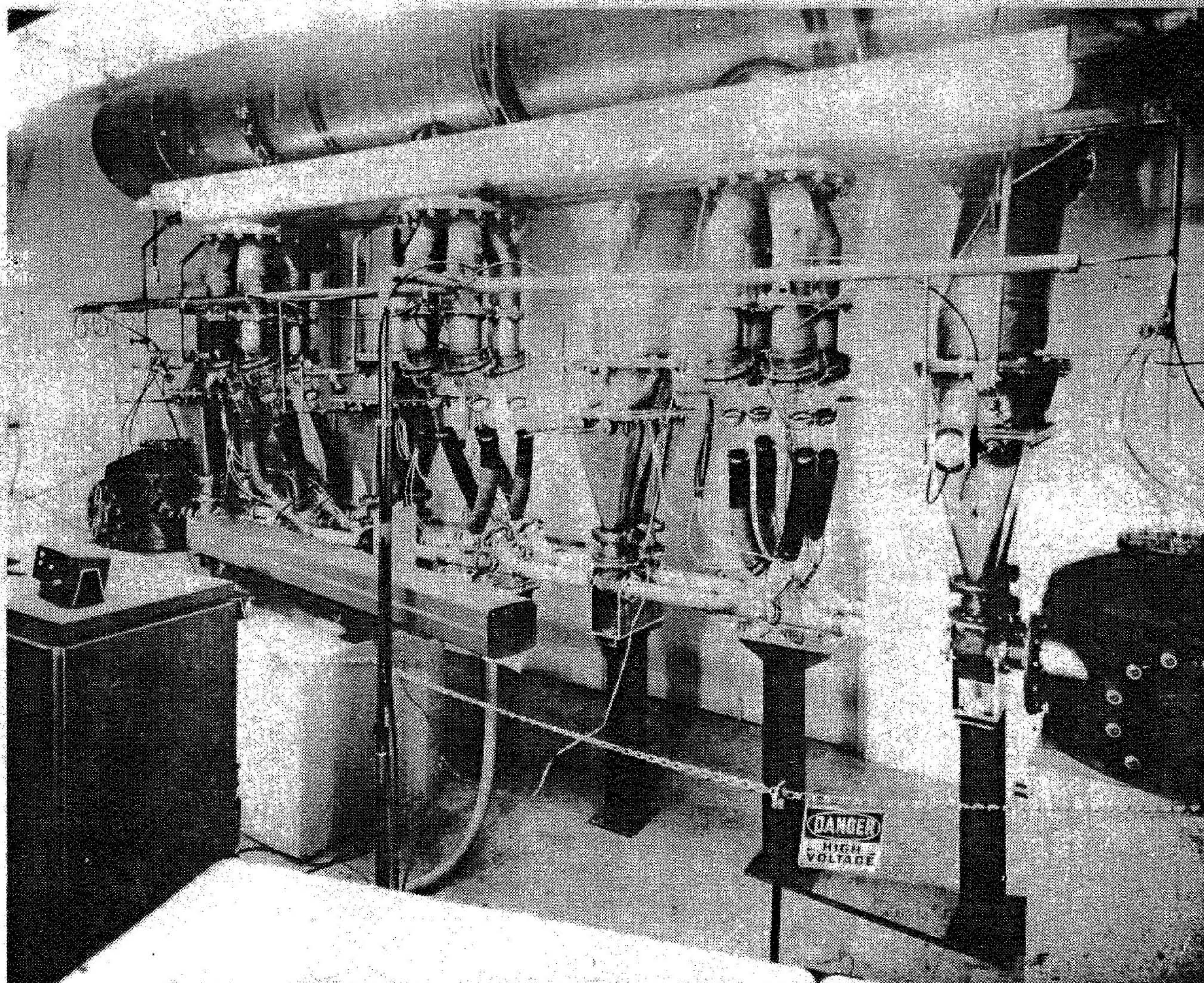

DEPTH OF FUSION VERSUS BEAM POWER DENSITY

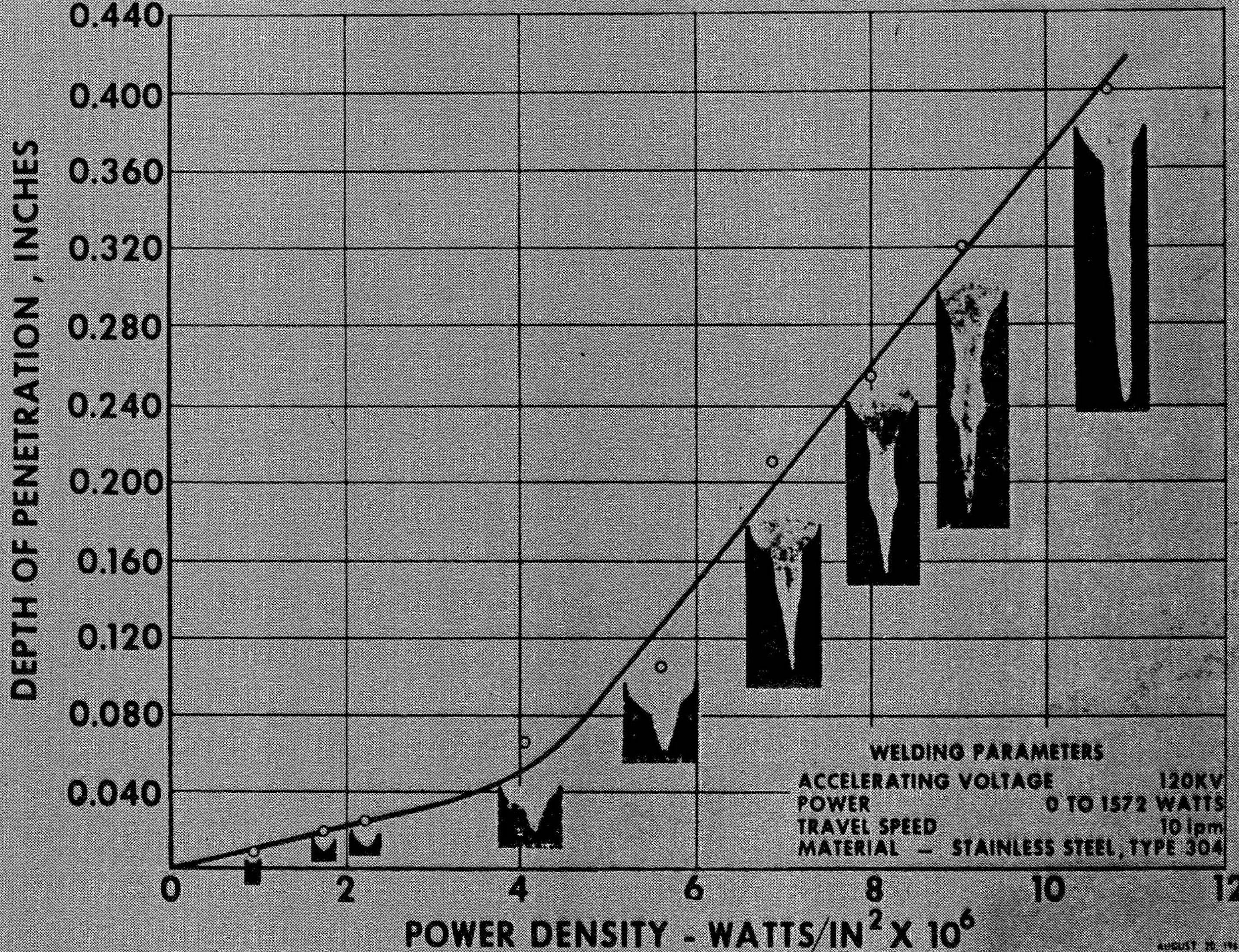

BEAM FOCUSING PARAMETERS

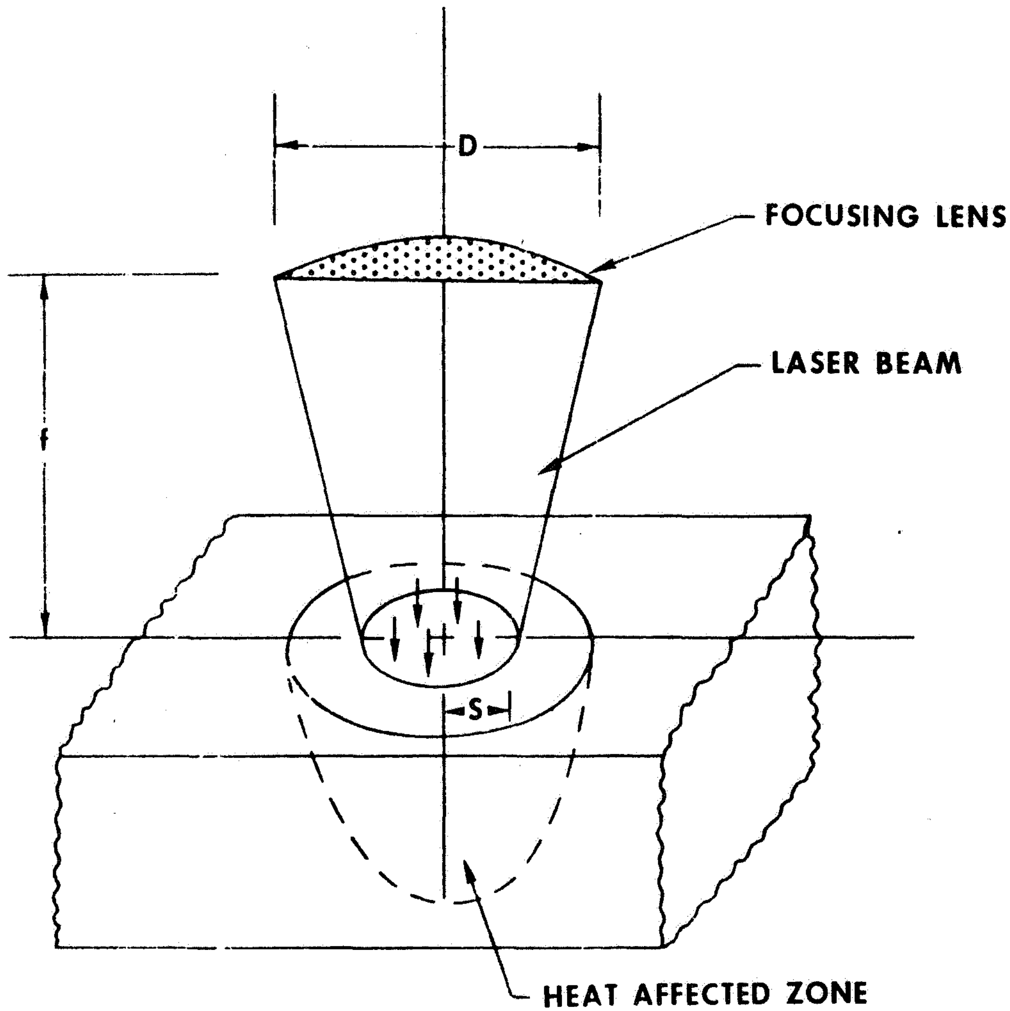

$$\text{POWER DENSITY} = K \cdot \frac{P_0}{\lambda^2} \cdot \frac{D^2}{f^2}$$

LASER INDUCED GAS BREAKDOWN

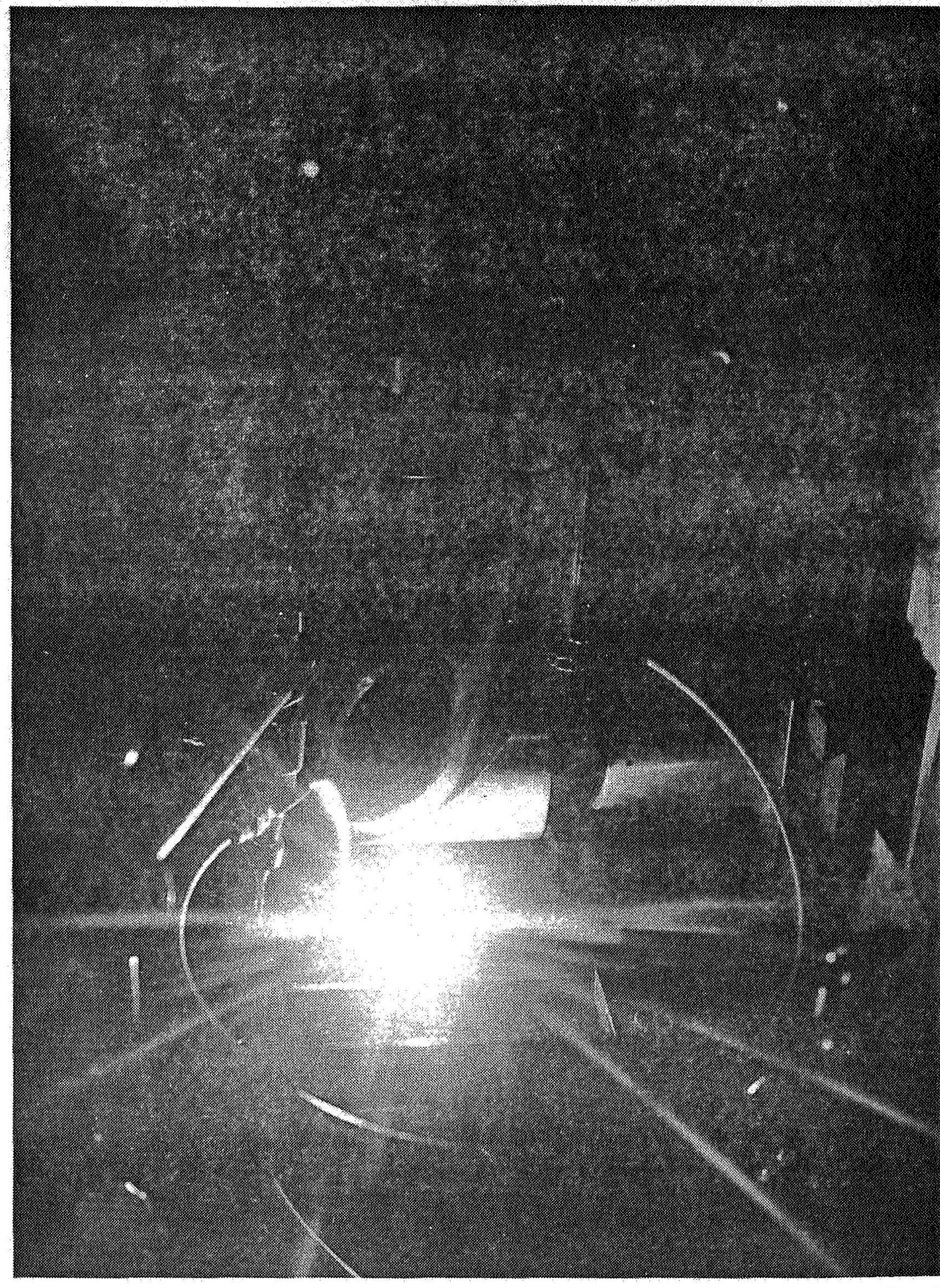

PLAN VIEW OF DEEP PENETRATION WELDING APPARATUS

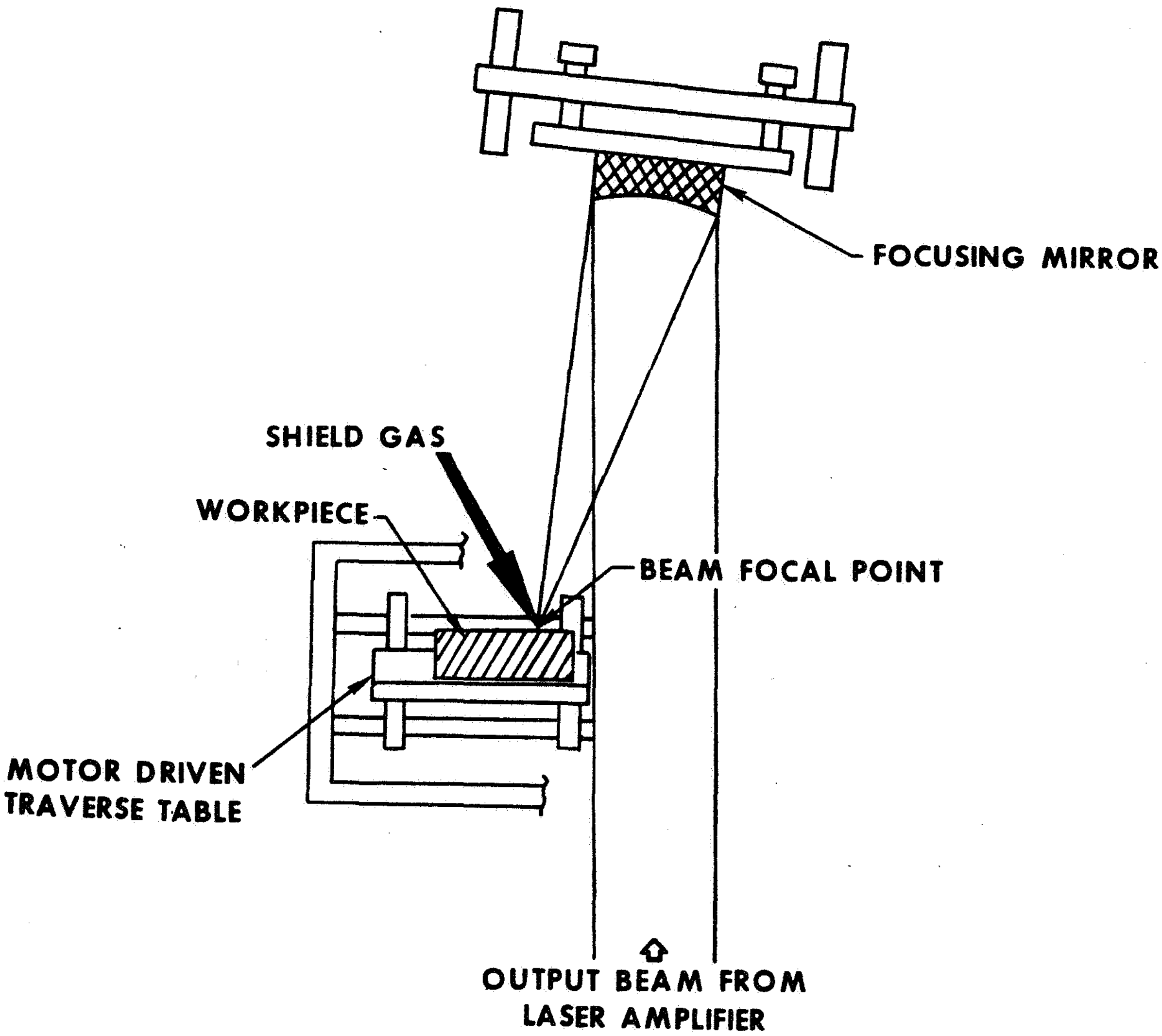

LASER BUTT WELD

LASER POWER: 3.5 KW | MATERIAL: STAINLESS STEEL

THICKNESS: 0.25 IN. | WELD SPEED: 50 IPM

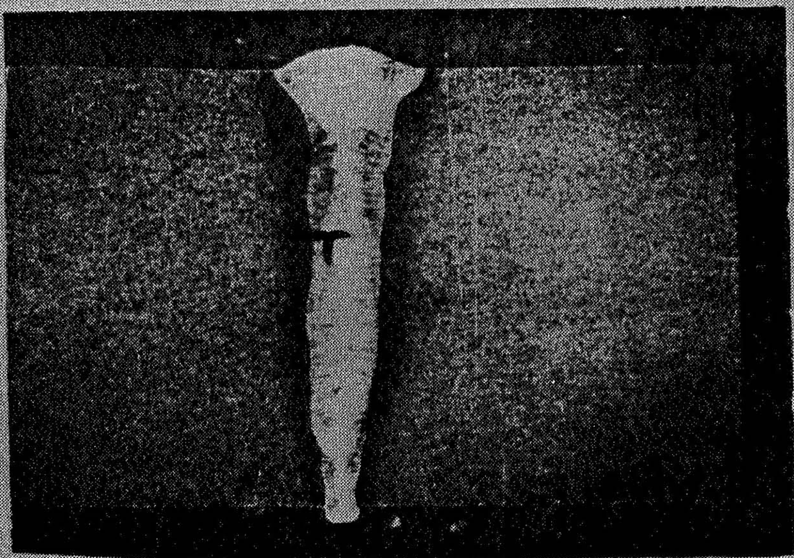

EFFECT OF LASER WELDING SPEED ON PENETRATION

STAINLESS STEEL

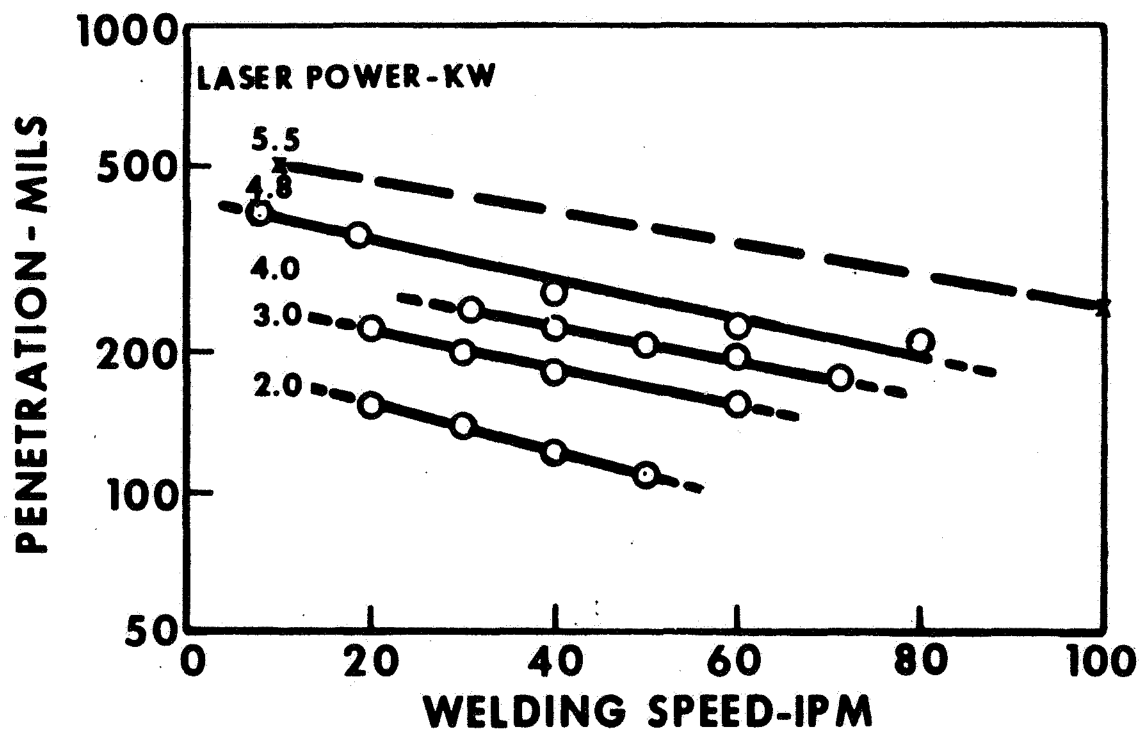

United Aircraft
Research Laboratories

EFFECT OF LASER WELDING SPEED ON PENETRATION

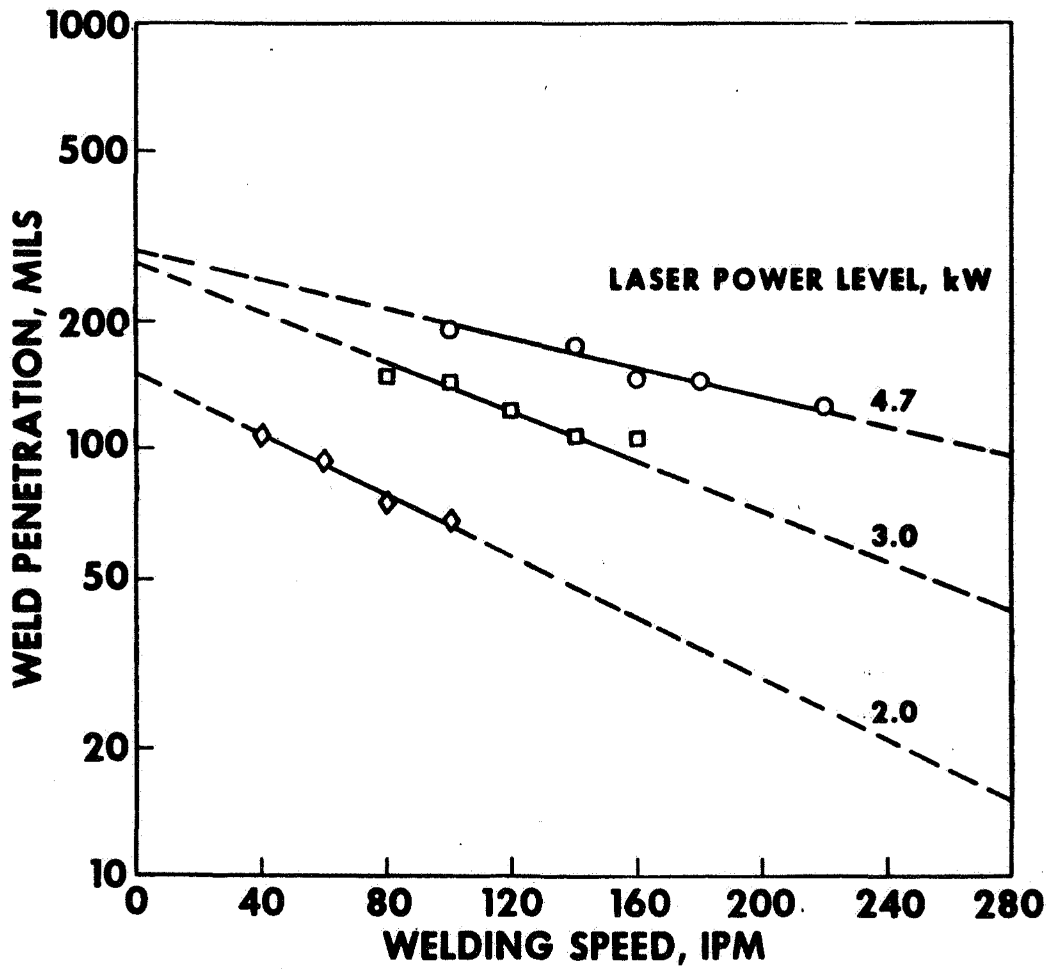

United Aircraft
Research Laboratories

>216<

EFFECT OF INERT GAS SHIELD ON RIMMED STEEL WELDS

4kW

200 IPM

0.5 IN

a. WITHOUT SHIELD

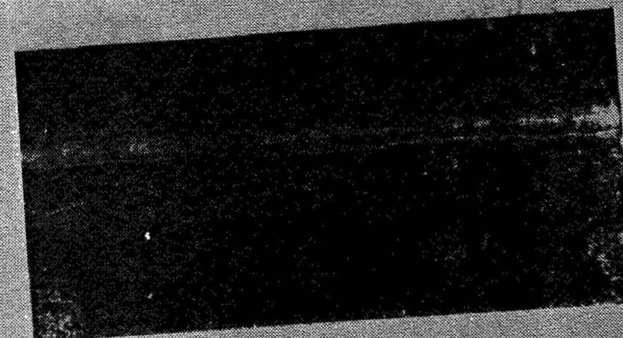

b. WITH SHIELD

EFFECT OF SPEED ON WELD CROSS SECTIONS

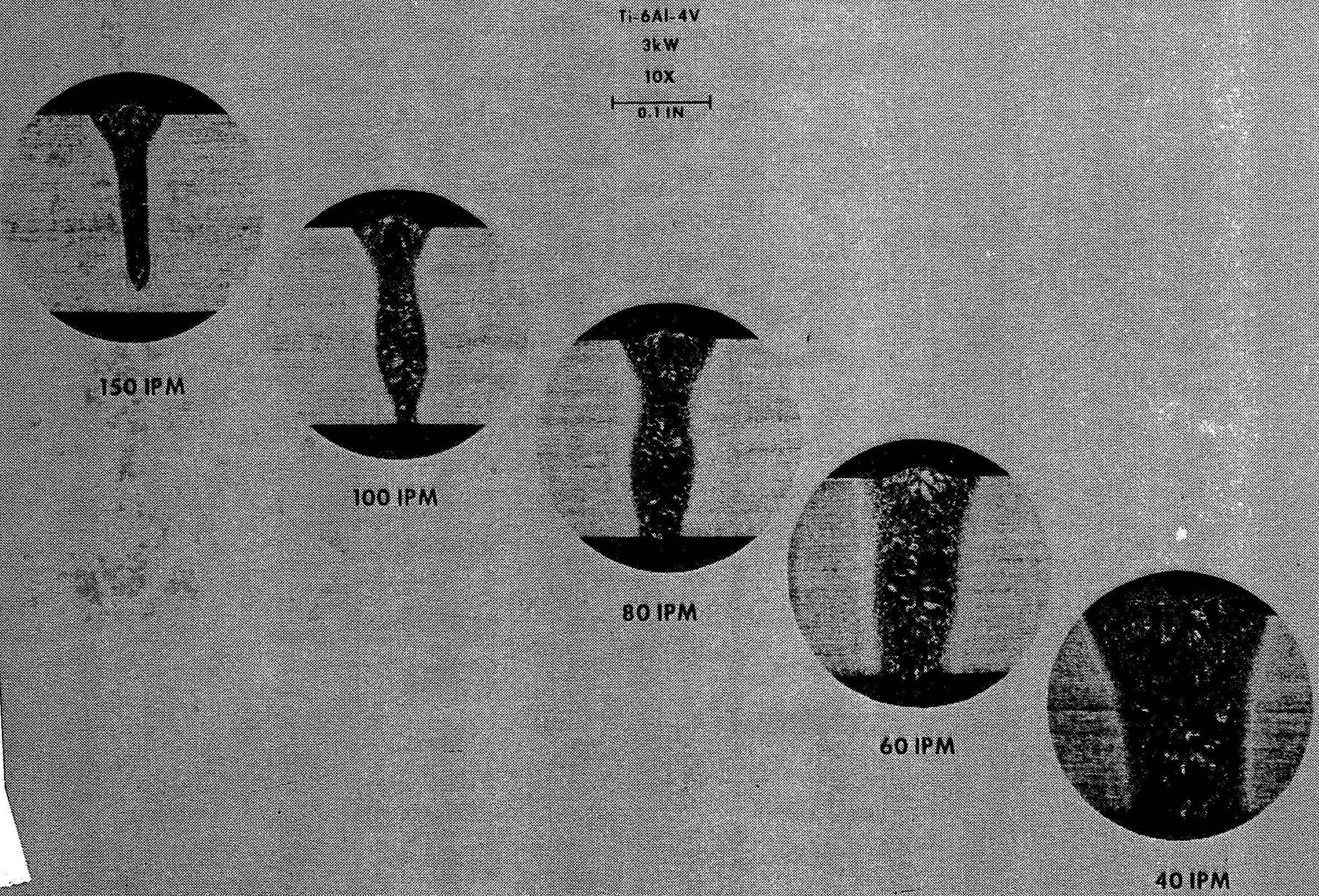

EFFECT OF SPEED ON WELD ZONE GRAIN STRUCTURE

3kW
Ti-6Al-4V

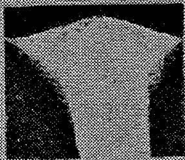

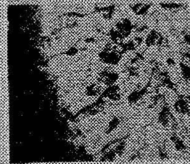

13 ×
0.1 IN

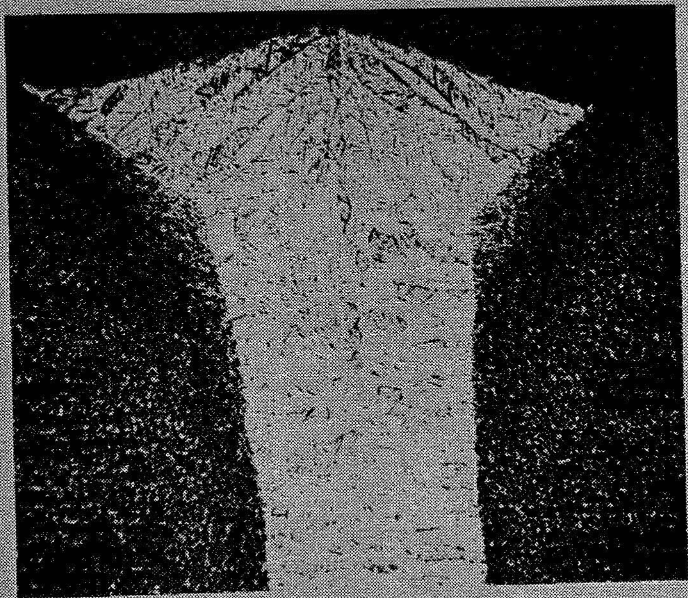

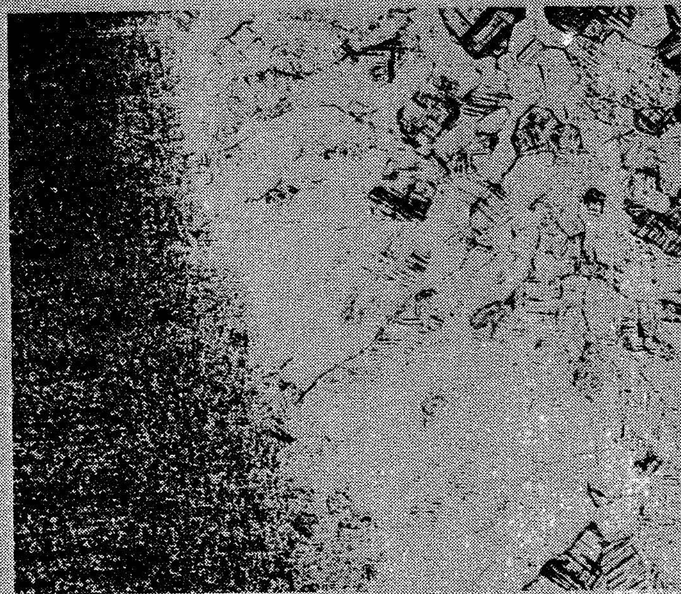

50×
0.02 IN

a. 200 IPM

b. 40 IPM

United Aircraft
Research Laboratories

EFFECT OF LASER WELDING SPEED ON PENETRATION

Ti-6Al-4V

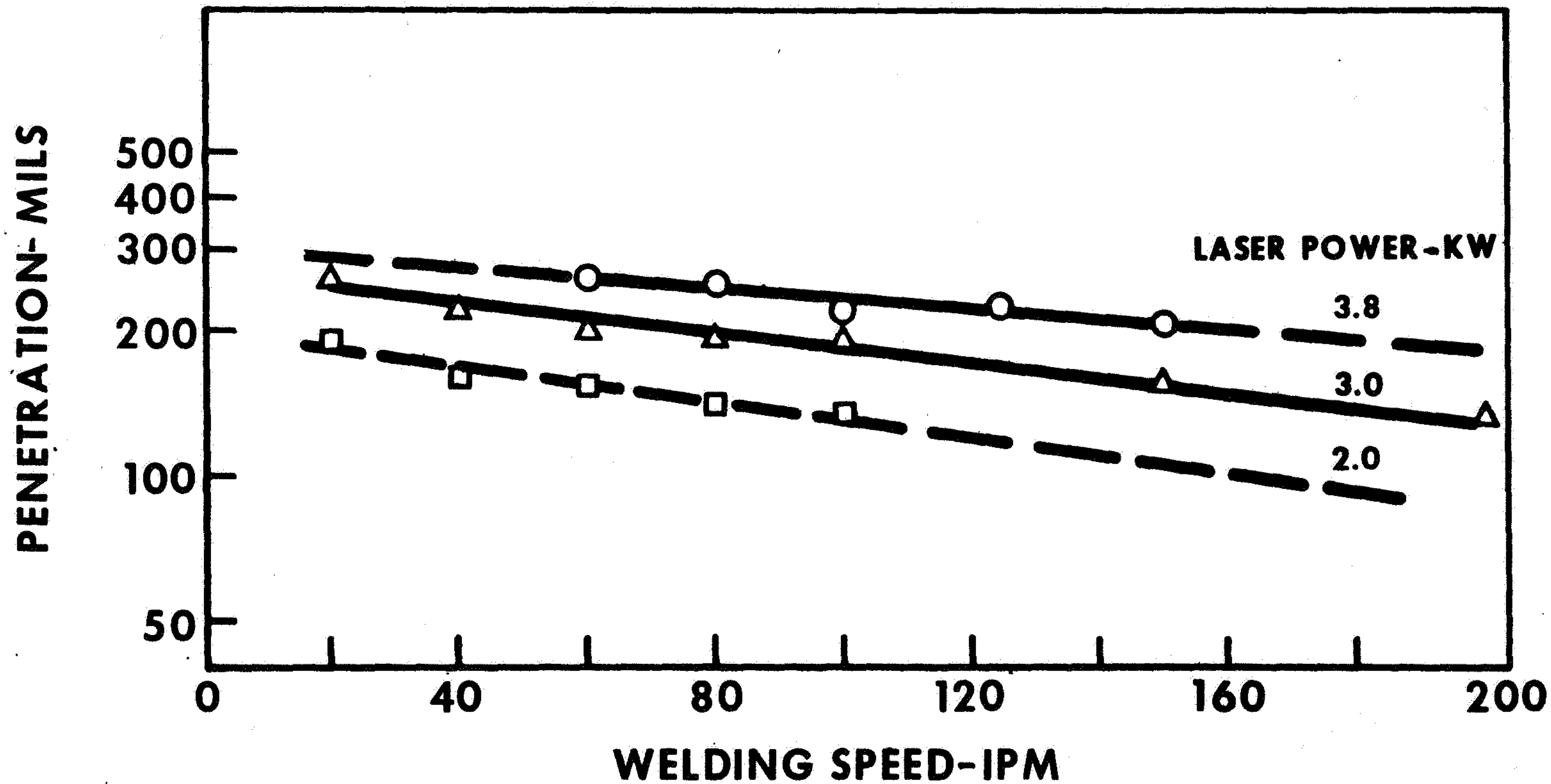

EFFECT OF POWER ON PENETRATION DEPTH

Ti-6Al-4V

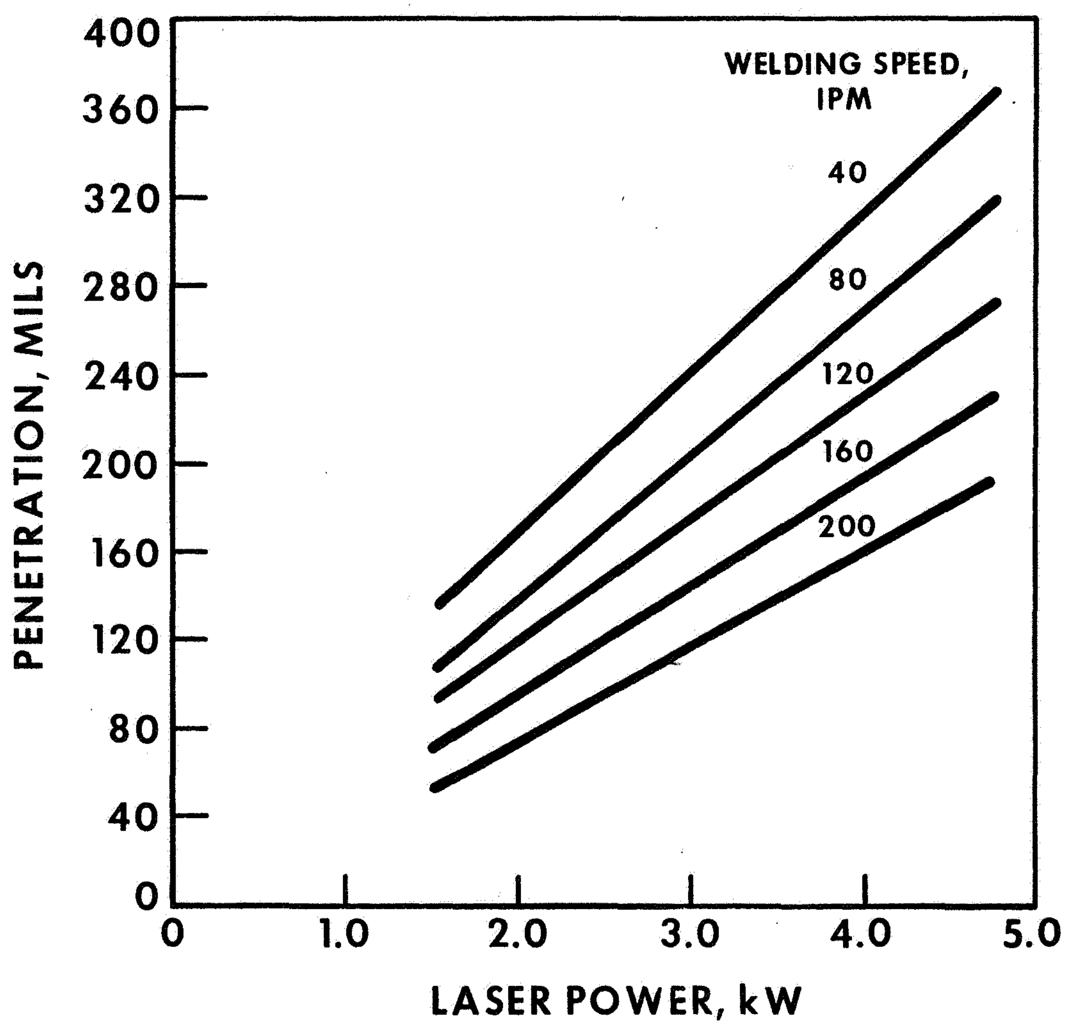

221

COMPARISON OF LASER AND ELECTRON BEAM WELDING PERFORMANCE